

On the rate of T_c suppression by the interband impurity scattering in MgB_2

Božidar Mitrović §

Physics Department, Brock University, St. Catharines, Ontario, Canada L2S 3A1

Abstract. We calculate the change in the superconducting transition temperature T_c of MgB_2 caused by interband nonmagnetic impurity scattering using the Eliashberg theory for the two-band model of this compound. Much slower rate of T_c suppression is obtained compared to the prediction based on the BCS treatment of the two-band model which ignores renormalization and damping associated with the electron-phonon interaction. Hence, the interband impurity scattering rates deduced from experiments on MgB_2 using the formula which results from the BCS approach to the two-band model are underestimated. We generalize the BCS treatment of the two-band model to include renormalization effects of the electron-phonon interaction and find an excellent agreement with the full strong coupling calculation.

PACS numbers: 74.20.-z, 74.70.Ad, 74.62.-c, 74.62.Dh

§ To whom correspondence should be addressed (mitrovic@brocku.ca)

1. Introduction

There is a large body of experimental [1-14] and theoretical (for a review see [15]) evidence that MgB_2 is a multiband superconductor which is well described by an effective two-band model [16]. In the case of a multiband superconductor one expects that the superconducting transition temperature T_c is reduced by the interband nonmagnetic (i.e. normal) impurity scattering in analogy to the effect of such scattering on anisotropic single band superconductors [17,18]. Several years before the discovery of superconductivity in MgB_2 the problem of impurity scattering in a multiband superconductor was examined in detail by Golubov and Mazin [19] using the weak coupling BCS-type treatment of the pairing interaction. They obtained an equation for the change in T_c with the interband impurity scattering rate which is analogous to the Abrikosov-Gor'kov formula for the T_c -suppression by paramagnetic impurity scattering in ordinary superconductors. The BCS-type treatment of Ref. [19] predicts that the T_c is reduced by about 40 % for the interband scattering rate comparable to $k_B T_c$. For MgB_2 that would imply a drop in T_c from 39 K to about 25 K for the interband impurity scattering rate $\Gamma \equiv 1/(2\tau) \equiv \gamma/2$ of about 1.7 meV. Thus, it was thought that observation of T_c suppression with increasing disorder would provide the final evidence for the two-band model of MgB_2 .

Experimentally, however, the situation appears to be more complicated. On one hand, as pointed out in [20], the transition temperatures of different samples of MgB_2 are rather insensitive to their respective residual resistivities : the T_c s of samples with residual resistivities in the range from 0.4 to 30 $\mu\Omega\text{cm}$ differ by at most 5%. On the other hand, irradiation of a polycrystalline sample of MgB_2 by fast neutrons led to an increase of residual resistivity and reduction in T_c by as much as 20% [13]. The apparent lack of correlation between T_c and residual resistivity in unirradiated samples was explained [20] by very small values of the interband impurity scattering matrix elements because of the particular electronic structure of MgB_2 so that the DC transport in this compound at low temperatures is primarily determined by *intraband* scattering which does not affect T_c [19], while very weak interband scattering leads to no significant change in T_c . The arguments in [20] apply to common substitutional impurities in MgB_2 which do not distort the lattice and subsequently Erwin and Mazin [21] proposed that substituting Mg with Al and/or Na would produce lattice distortions that could lead to large enough interband impurity scattering rates to cause a reduction of T_c by a couple of degrees as predicted theoretically in [19]. Presumably the irradiation by fast neutrons generates enough lattice distortions to cause a 20% drop in T_c [13].

Nevertheless, the break junction tunneling experiments on MgB_2 [4] clearly indicate that the interband impurity scattering is significant even in undoped and unirradiated samples. Namely, the only justification for using the equations of McMillan tunneling model for proximity effect [22] in analyzing the break junction data on MgB_2 is provided by the work of Schopohl and Scharnberg [23] on tunneling density of states of a disordered two-band superconductor. The fact that in the latter case the equations

have the form identical to those of the McMillan tunneling model for proximity effect is a pure accident as is evident from the entirely different meaning of the quasiparticle scattering rates in the two cases. The interband scattering rates used to fit the tunneling data [4] were at least as large as those predicted for Al/Na doped MgB_2 (Γ s were in the range from 1 to 4 meV), but the T_c of the material was reported to be 39 K - close to the maximum value for MgB_2 of 39.4 K. A possible solution to this contradiction is that the weak coupling BCS-type treatment of impurity scattering in a multiband superconductor used in [19] is not *quantitatively* accurate for MgB_2 . The calculated electron-phonon interactions in MgB_2 [16] indicate that it is a medium-to-strong coupling superconductor (the largest calculated electron-phonon parameter $\lambda_{\sigma\sigma}$ for σ -band electrons is comparable to the one in Nb) and renormalization and damping effects could play an important role in determining the rate of T_c suppression by interband impurity scattering.

In section 2 we solve the Eliashberg equations for a two-band superconductor with nonmagnetic impurity scattering and calculate the transition temperature as a function of the impurity scattering rate using realistic interaction parameters for MgB_2 [16,24]. We find that the T_c is suppressed by interband scattering at much slower rate than what was obtained using the BCS treatment in Ref. [19]. In the same section we present the functional derivatives $\delta T_c / \delta \alpha^2 F_{ij}$, $i, j = \sigma, \pi$ [25] for several representative impurity interband scattering rates which show how the sensitivity of T_c to various electron-phonon couplings changes with impurity scattering. In section 3 we generalize the BCS approach to include the renormalization caused by the electron-phonon interaction by extending the well known θ - θ model [26] to the two-band case. The numerical solution of such a model is found to be in excellent agreement with the full strong coupling calculation. In section 4 we give a summary.

2. Strong coupling calculation

2.1. Formalism

The Eliashberg equations for T_c of a superconductor with several isotropic bands $i = 1, 2, \dots$ which include nonmagnetic impurity scattering described by the Born approximation are [25,26]

$$\phi_i(n) = \phi_i^0(n) + \sum_j \frac{1}{2\tau_{ij}} \frac{\phi_j(n)}{|\omega_n| Z_j(n)}, \quad (1)$$

$$\phi_i^0(n) = \pi T_c \sum_j \sum_{m=-\infty}^{+\infty} [\lambda_{ij}(n-m) - \mu_{ij} \theta(E_F - |\omega_m|)] \frac{\phi_j(m)}{|\omega_m| Z_j(m)}, \quad (2)$$

$$\omega_n Z_i(n) = \omega_n Z_i^0(n) + \sum_j \frac{1}{2\tau_{ij}} \frac{\omega_n}{|\omega_n|}, \quad (3)$$

$$\omega_n Z_i^0(n) = \omega_n + \pi T_c \sum_j \sum_{m=-\infty}^{+\infty} \lambda_{ij}(n-m) \frac{\omega_m}{|\omega_m|}. \quad (4)$$

Here $\phi_i(n)$ is the pairing self-energy in the band i at the Matsubara frequency $\omega_n = \pi T_c(2n-1)$ and $Z_i(n)$ is the corresponding renormalization function (for a review of the Eliashberg theory of superconducting T_c see [26]). The part $\phi_i^0(n)$, Eq. (2), results from the intraband and interband electron-phonon and screened Coulomb interactions, while the second term in Eq. (1) represents the impurity scattering contribution. In the same way, $Z_i^0(n)$ is the contribution to the renormalization function from the intraband and interband electron-phonon interaction and the second term in Eq. (3) gives the impurity contribution to $Z_i(n)$. The cutoff E_F on the sums over the Matsubara frequencies ω_m in Eq. (2) is initially taken to be large enough so that the Coulomb repulsion parameters are given by $\mu_{ij} = V_{ij}^c N_j$, where V_{ij}^c is the Fermi surface averaged screened Coulomb matrix element between the states in the bands i and j ($V_{ij}^c = V_{ji}^c$) and N_j is the Fermi surface density of states in band j [25]. The electron-phonon coupling functions $\alpha^2 F_{ij}(\Omega) = \alpha^2 f_{ij}(\Omega) N_j$ ($\alpha^2 f_{ij}(\Omega) = \alpha^2 f_{ji}(\Omega)$) enter via parameters $\lambda_{ij}(n-m)$

$$\lambda_{ij}(n-m) = \int_0^{+\infty} d\Omega \alpha^2 F_{ij}(\Omega) \frac{2\Omega}{\Omega^2 + (\omega_n - \omega_m)^2}, \quad (5)$$

and the impurity scattering rates $\gamma_{ij} \equiv 1/\tau_{ij}$ are given by (we use the units in which $\hbar=1$ and the Boltzmann's constant $k_B=1$)

$$\frac{1}{2\tau_{ij}} = n_{imp} \pi N_j |V_{ij}|^2 \quad (6)$$

where n_{imp} is the concentration of nonmagnetic impurities and V_{ij} is the Fermi surface averaged matrix element of the change in the lattice potential caused by an impurity between the states in the bands i and j . Clearly, $\gamma_{ij}/\gamma_{ik} = N_j/N_k = \lambda_{ij}/\lambda_{ik}$, where $\lambda_{ij} = \lambda_{ij}(0)$ (see equation (5)).

In principle, Eqs. (1)-(4) have the form of an eigenvalue problem of a temperature dependent matrix with eigenvector $\hat{\phi}$, and T_c is determined as the highest temperature at which the largest eigenvalue of the matrix is one. However, before such solution is attempted one can simplify the problem further. First, by introducing the gap function as renormalized pairing self-energy $\Delta_i(n) = \phi_i(n)/Z_i(n)$ one can eliminate the *intraband* impurity scattering from the problem by combining Eqs. (1) and (3)

$$\Delta_i(n) \left(Z_i^0(n) + \sum_{j \neq i} \frac{1}{2\tau_{ij}} \frac{1}{|\omega_n|} \right) = \phi_i^0(n) + \sum_{j \neq i} \frac{1}{2\tau_{ij}} \frac{\Delta_j(n)}{|\omega_n|}, \quad (7)$$

where $\phi_i^0(n)$ is given by Eq. (2) with $\phi_j(m)/Z_j(m)$ replaced by $\Delta_j(m)$. Next, the eigenvalue problem can be symmetrized by defining

$$u_i(n) = \sqrt{N_i} \frac{\Delta_i(n)}{|\omega_n|} \sqrt{|\omega_n| Z_i^0(n) + \sum_{j \neq i} \frac{1}{2\tau_{ij}}} \quad (8)$$

together with $\lambda_{ij}^s(n-m) = \sqrt{N_i/N_j} \lambda_{ij}(n-m)$, $\mu_{ij}^s = \sqrt{N_i/N_j} \mu_{ij}$ and $1/(2\tau_{ij}^s) = \sqrt{N_i/N_j}/(2\tau_{ij})$. With these definitions Eq. (7) reduces to

$$u_i(n) = \varepsilon(T) \sum_j \sum_{m=-\infty}^{\infty} \pi T \frac{\lambda_{ij}^s(n-m) - \mu_{ij}^s \theta(E_F - |\omega_m|) + \frac{1}{2\pi T \tau_{ij}^s} (1 - \delta_{ij}) \delta_{nm}}{\sqrt{|\omega_n| Z_i'(n)} \sqrt{|\omega_m| Z_j'(m)}} u_j(m), \quad (9)$$

with

$$Z'_i(n) = Z_i^0(n) + \sum_{j \neq i} \frac{1}{2\tau_{ij}} \frac{1}{|\omega_n|} \quad (10)$$

and $\varepsilon(T)=1$ when $T = T_c$. Finally, the size of the matrix which has to be diagonalized can be reduced by cutting off the Matsubara sums in (9) at a smaller energy ω_c which is still large enough so that $Z'_i(n) \approx 1$ for $|\omega_n| > \omega_c$; hence, ω_c has to be at least 5-10 times the maximum phonon energy Ω_m in various spectral functions $\alpha^2 F_{ij}(\Omega)$ and much larger than the largest band off-diagonal $1/2\tau_{ij}$. The reduction in cutoff from E_F to ω_c is accompanied by replacement of the Coulomb repulsion parameters μ_{ij}^s in (9) with $\mu_{ij}^*(\omega_c)$ where the matrix (in band indices) $\hat{\mu}^*(\omega_c)$ is related to matrix $\hat{\mu}^s$ by [25]

$$\hat{\mu}^*(\omega_c) = \left(\hat{1} + \hat{\mu}^s \ln \frac{E_F}{\omega_c} \right)^{-1} \hat{\mu}^s. \quad (11)$$

2.2. Numerical Results

We solved Eqs. (9)-(11) using the spectral functions $\alpha^2 F_{\sigma\sigma}$, $\alpha^2 F_{\sigma\pi}$, $\alpha^2 F_{\pi\pi}$ and $\alpha^2 F_{\pi\sigma}$ for MgB_2 obtained from the first principle electronic structure calculations and presented in [16]. The corresponding coupling parameters given by Eq. (5) with $\omega_n - \omega_m = 0$ are $\lambda_{\sigma\sigma} = 1.017$, $\lambda_{\sigma\pi} = 0.212$, $\lambda_{\pi\pi} = 0.446$ and $\lambda_{\pi\sigma} = 0.155$. Since $\alpha^2 F_{ij}(\Omega) = \alpha^2 f_{ij}(\Omega) N_j$, with $\alpha^2 f_{ij}(\Omega) = \alpha^2 f_{ji}(\Omega)$, these values of λ -parameters fix the ratio of the partial band densities of states $N_\pi/N_\sigma = \lambda_{\sigma\pi}/\lambda_{\pi\sigma}$ at 1.37. That fixes the ratio $\gamma_{\sigma\pi}/\gamma_{\pi\sigma}$ (see Eq. (6)) and we chose $\gamma_{\pi\sigma}$ as the independent scattering parameter.

To minimize the effect of changes in the number $N_c = [\omega_c/(2\pi T_c) + 0.5]$ of Matsubara frequencies ($[\dots]$ denotes the integer part) on our numerical results as T_c is reduced by increased interband impurity scattering rate we had to take the cutoff ω_c to be at least 10 times the maximum phonon energy Ω_m . With ω_c fixed at 1000 meV the Coulomb repulsion parameters $\mu_{\sigma\sigma}^*$, $\mu_{\sigma\pi}^*$, $\mu_{\pi\pi}^*$, $\mu_{\pi\sigma}^*$ were determined as follows. Choi *et al.* [24] calculated the ratios of the *screened* Coulomb repulsion parameters for MgB_2 to be $\mu_{\sigma\sigma} : \mu_{\pi\pi} : \mu_{\sigma\pi} : \mu_{\pi\sigma} = 1.75 : 2.04 : 1.61 : 1.00$. Since $\mu_{ij} = V_{ij}^c N_j$, the ratio $\mu_{\sigma\pi}/\mu_{\pi\sigma} = 1.61$ implies that in their calculation $N_\pi/N_\sigma = 1.61$, which is considerably higher than the value of 1.37 found in [16] and adopted by us in this work by our choice of the electron-phonon coupling spectra. Leaving aside the reasons for such a discrepancy in N_π/N_σ between the two sets of electronic structure calculations we use the ratios of the μ -values calculated in [24] to extract from them the ratios of the *screened* Coulomb matrix elements: $V_{\sigma\sigma}^c : V_{\pi\pi}^c = 1.75 : 1.00$, $V_{\sigma\pi}^c : V_{\pi\sigma}^c = 2.04 : 1.61$ and, because $V_{\pi\sigma}^c = V_{\sigma\pi}^c$, $V_{\sigma\sigma}^c : V_{\pi\pi}^c = 1.75 : 1.267$. These could be combined with $N_\pi/N_\sigma = 1.37$ to produce the ratios $\mu_{\sigma\sigma}/\mu_{\pi\pi} = 1.01$, $\mu_{\sigma\sigma}/\mu_{\sigma\pi} = 1.28$ and $\mu_{\sigma\sigma}/\mu_{\pi\sigma} = 1.75$ leaving the single fitting parameter $\mu_{\sigma\sigma}$ once a choice is made for the initial cutoff E_F (see Eq. (11)). Since E_F is on the order of the largest electronic energy scale in the problem, we took E_F to be equal to the π -bandwidth of 15 eV [27] and fitted $\mu_{\sigma\sigma}$ in the four equations implied by the 2×2 matrix equation (11)

$$\mu_{\sigma\sigma}^*(\omega_c) = \left[\mu_{\sigma\sigma} + (\mu_{\sigma\sigma}\mu_{\pi\pi} - \mu_{\sigma\pi}\mu_{\pi\sigma}) \ln \frac{E_F}{\omega_c} \right] / D, \quad (12)$$

$$\mu_{\sigma\pi}^*(\omega_c) = \sqrt{N_\sigma/N_\pi} \mu_{\sigma\pi}/D, \quad (13)$$

$$\mu_{\pi\pi}^*(\omega_c) = \left[\mu_{\pi\pi} + (\mu_{\sigma\sigma}\mu_{\pi\pi} - \mu_{\sigma\pi}\mu_{\pi\sigma}) \ln \frac{E_F}{\omega_c} \right] / D, \quad (14)$$

$$(15)$$

$$D = 1 + (\mu_{\sigma\sigma} + \mu_{\pi\pi}) \ln \frac{E_F}{\omega_c} (\mu_{\sigma\sigma}\mu_{\pi\pi} - \mu_{\sigma\pi}\mu_{\pi\sigma}) \left(\ln \frac{E_F}{\omega_c} \right)^2, \quad (16)$$

to the experimental T_{c0} of 39.4 K for the case of no impurity scattering. The results were $\mu_{\sigma\sigma} = 0.848234$ with $\mu_{\sigma\sigma}^*(\omega_c) = 0.225995$, $\mu_{\pi\pi}^*(\omega_c) = 0.225010$ and $\mu_{\sigma\pi}^*(\omega_c) = \mu_{\pi\sigma}^*(\omega_c) = 0.067148$.

In Figure 1 we show with the solid line the calculated T_c/T_{c0} as a function of $\gamma_{\pi\sigma}/T_{c0}$ (note that for $\gamma_{\pi\sigma}/T_{c0} \geq 2$ the scale is logarithmic). The dotted line represents the prediction based on the BCS weak coupling approach of Ref. [19] where T_c drops initially with the slope $-\pi/8$ (see Fig. 1 and Eq. (13) in [19]). Clearly the full strong coupling calculation with realistic electron-phonon spectral functions and Coulomb repulsion parameters leads to a much slower drop in T_c with increasing interband impurity scattering rate than what was obtained in [19] using the BCS approach: for $\gamma_{\pi\sigma} = T_{c0}$ we get a drop in transition temperature of only 8 %, while the BCS treatment predicts a drop of about 36 %.

Before we address in the next section the reasons for such a large discrepancy between the strong coupling and the BCS results we give in Figs. (2) and (3) calculated functional derivatives $\delta T_c / \delta \alpha^2 F_{ij}$, $i, j = \sigma, \pi$ which show how the sensitivity of T_c to various electron-phonon couplings changes with increasing interband impurity scattering. In [25] these functional derivatives were computed for the case of no impurity scattering and it was found that the band-diagonal functional derivatives $\delta T_c / \delta \alpha^2 F_{\sigma\sigma}$ and $\delta T_c / \delta \alpha^2 F_{\pi\pi}$ have similar shapes but their overall magnitudes differ due to difference in sizes of the gap-functions $\Delta_\sigma(n)$ and $\Delta_\pi(n)$ in the two bands. This is also the case for the lowest $\gamma_{\pi\sigma}$ in Fig. 2, but as the scattering rate increases the difference in magnitudes of the two gaps becomes smaller and the overall magnitudes of the two band-diagonal functional derivatives become comparable. For $\gamma_{\pi\sigma} = 100T_{c0}$ the magnitude of $\delta T_c / \delta \alpha^2 F_{\pi\pi}$ is larger than the magnitude of $\delta T_c / \delta \alpha^2 F_{\sigma\sigma}$ presumably because $\lambda_{\pi\pi} < \lambda_{\sigma\sigma}$ [28] and the difference in sizes of the gaps $\Delta_\sigma(n)$ and $\Delta_\pi(n)$ has largely disappeared. Another consequence of this disappearance of the difference between the gaps in the two bands is that with increasing $\gamma_{\pi\sigma}$ the shapes of $\delta T_c / \delta \alpha^2 F_{\pi\sigma}$ and $\delta T_c / \delta \alpha^2 F_{\sigma\pi}$, Fig. 3, become more and more similar to the shapes of the band-diagonal functional derivatives. The divergencies at $\Omega = 0$ still persist, but are progressively confined to smaller and smaller neighborhoods of $\Omega = 0$. Again, the local maximum in $\delta T_c / \delta \alpha^2 F_{\pi\sigma}$ near $\Omega = 8k_B T_c$ for $\gamma_{\pi\sigma} = 100T_{c0}$ is higher than the corresponding maximum in $\delta T_c / \delta \alpha^2 F_{\sigma\pi}$ because $\lambda_{\pi\sigma} < \lambda_{\sigma\pi}$ [28].

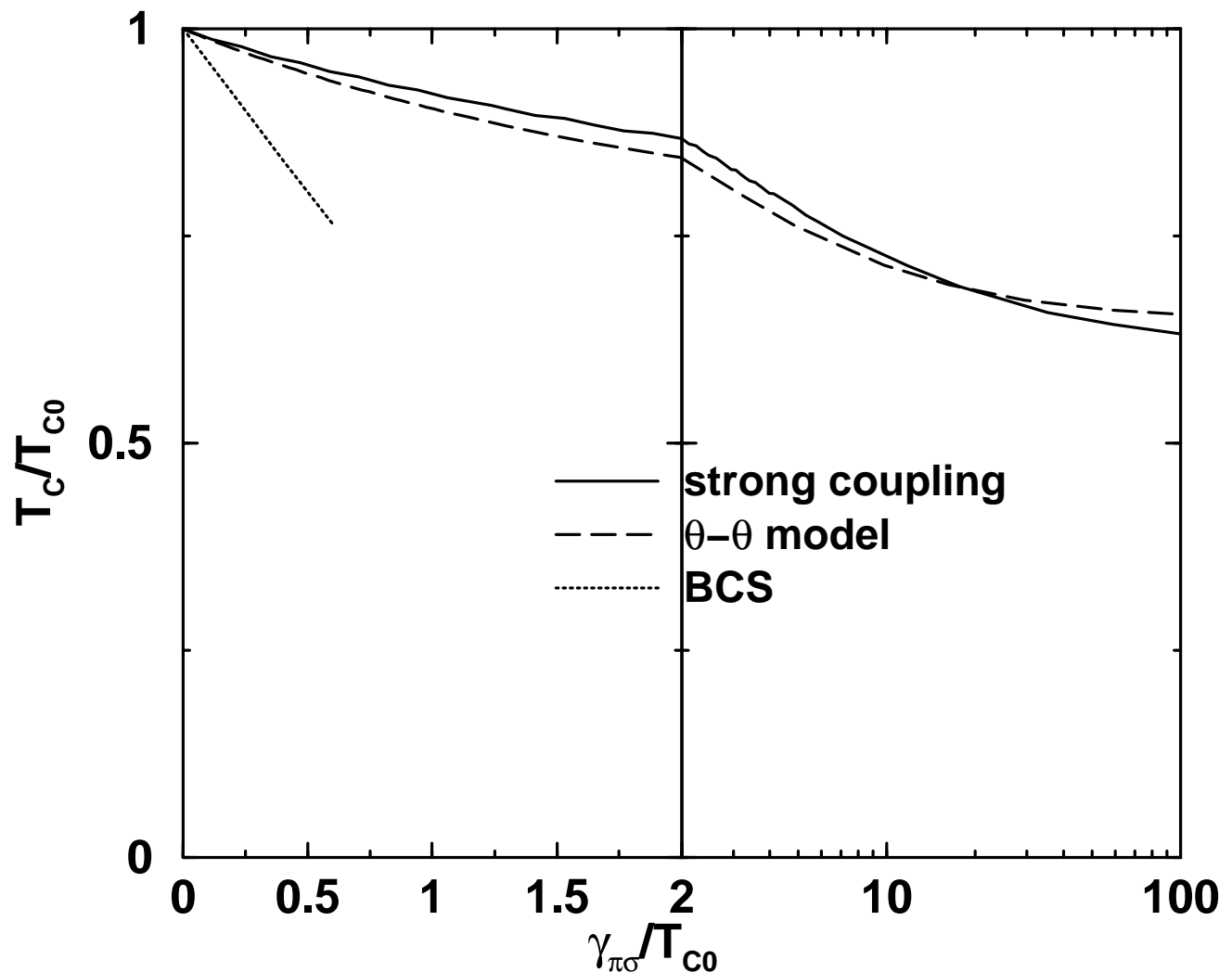


Figure 1. The relative change in the transition temperature T_c/T_{c0} as a function of the interband impurity scattering rate parameter $\gamma_{\pi\sigma}/T_{c0}$. The solid curve gives the results of the full strong coupling calculation for MgB_2 and the long dashed curve gives the results obtained from θ - θ model with interaction parameters that were used in the strong coupling calculation. The dotted line indicates the weak coupling result from Ref. [19] which predicts for low values of $\gamma_{\pi\sigma}$ a straight line with the slope $-\pi/8$.

3. θ - θ model calculation

The main difference between the strong coupling Eliashberg theory and the BCS approach is that the latter does not include the renormalization and the damping effects associated with the electron-phonon interaction. In the BCS calculation $Z_i^0(n)$, Eq. (4), is set equal to 1. It is possible to improve upon the BCS approach so that the effects of renormalization by electron-phonon interaction are included in an approximate way through so-called θ - θ model [26]. In this model $\lambda_{ij}(n-m)$ in Eq. (2) for the electron-

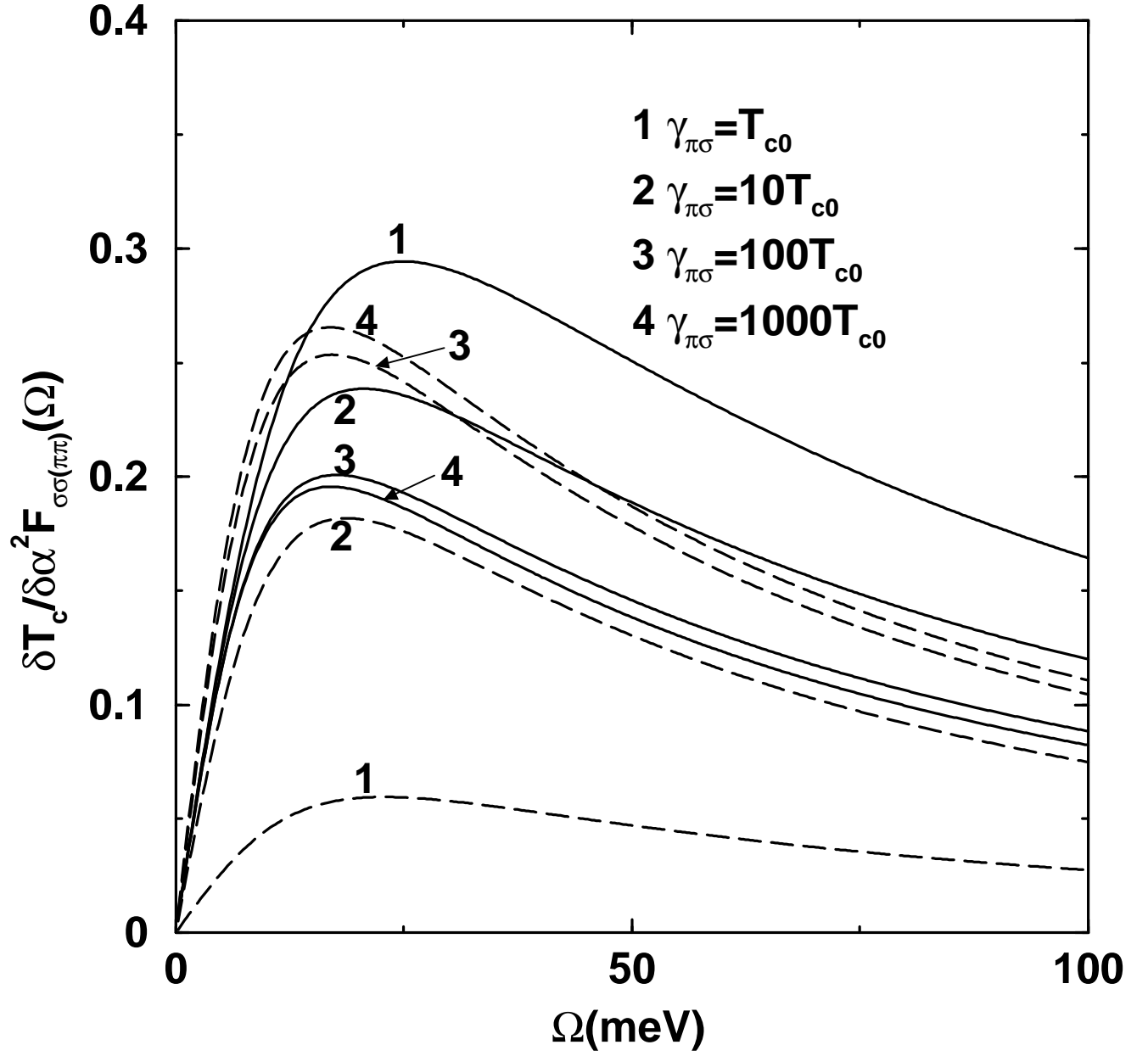


Figure 2. The band-diagonal functional derivatives $\delta T_c / \delta \alpha^2 F_{\sigma\sigma}$ (solid lines) and $\delta T_c / \delta \alpha^2 F_{\pi\pi}$ (long dashed lines) for four different values of $\gamma_{\pi\sigma}$ given in units of T_{c0} .

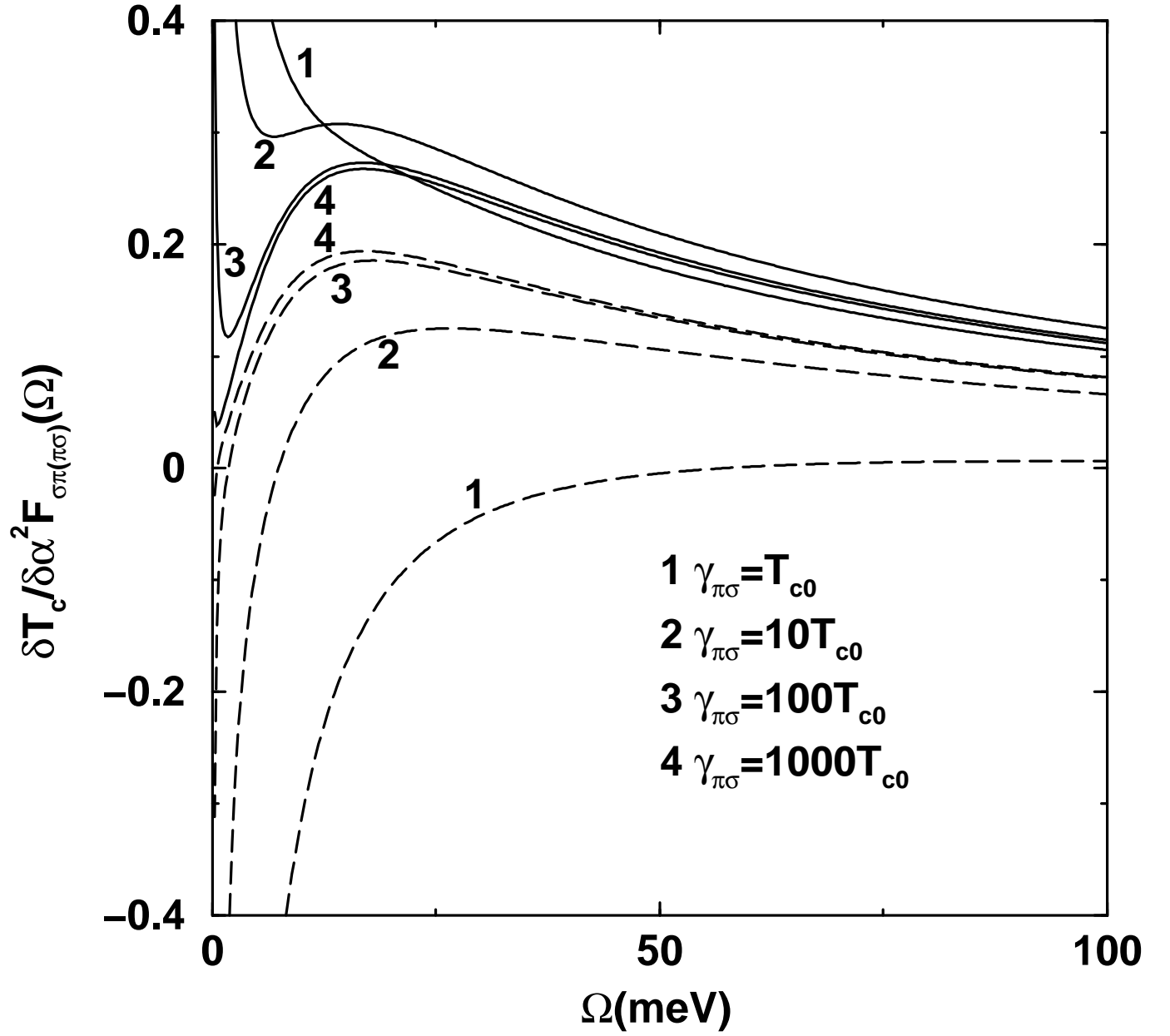


Figure 3. The band-off-diagonal functional derivatives $\delta T_c / \delta \alpha^2 F_{\pi\sigma}$ (solid lines) and $\delta T_c / \delta \alpha^2 F_{\sigma\pi}$ (long dashed lines) for four different values of $\gamma_{\pi\sigma}$ given in units of T_{c0} .

phonon contribution to the pairing self-energy is replaced by $\lambda_{ij}\theta(\Omega_m - |\omega_n|)\theta(\Omega_m - |\omega_m|)$ with Ω_m - the maximum phonon energy (BCS approximation) and, after rewriting the sum in (4) as

$$\sum_{m=-\infty}^{+\infty} \lambda_{ij}(n-m) \frac{\omega_m}{|\omega_m|} = 2 \sum_{m=1}^{n-1} \lambda_{ij}(m) - \lambda_{ij}(0),$$

$\lambda_{ij}(m)$ in Eq. (4) for the electron-phonon contribution to the renormalization function is replaced by $\lambda_{ij}\theta(\Omega_m - |\omega_m|)$. After rescaling the Coulomb repulsion matrix from cutoff ω_c to Ω_m according to the general prescription (11), i.e. $\hat{\mu}^*(\Omega_m) = [\hat{1} + \hat{\mu}^*(\omega_c) \ln(\omega_c/\Omega_m)]^{-1} \hat{\mu}^*(\omega_c)$ one gets instead of (7)

$$\begin{aligned} \Delta_i(n) \left(1 + \sum_j \lambda_{ij} + \sum_{j \neq i} \frac{1}{2\tau_{ij}} \frac{1}{|\omega_n|} \right) &= \sum_{j, |\omega_m| \leq \Omega_m} (\lambda_{ij} - \mu_{ij}^*(\Omega_m)) \pi T_c \frac{\Delta_j(m)}{|\omega_m|} \\ &+ \sum_{j \neq i} \frac{1}{2\tau_{ij}} \frac{\Delta_j(n)}{|\omega_n|}, \end{aligned} \quad (17)$$

for $|\omega_n| \leq \Omega_m$. After defining

$$\delta_{in} = \sqrt{N_i} \frac{\Delta_i(n)}{|\omega_n|} \sqrt{1 + \sum_j \lambda_{ij}}, \quad (18)$$

$$\Lambda_{ij} = \frac{\sqrt{N_i/N_j} \lambda_{ij} - \mu_{ij}^*(\Omega_m)}{\sqrt{1 + \sum_k \lambda_{ik}} \sqrt{1 + \sum_k \lambda_{jk}}}, \quad (19)$$

$$G_{ij} = \frac{1/(2\pi T_c t_{ij})}{\sqrt{1 + \sum_k \lambda_{ik}} \sqrt{1 + \sum_k \lambda_{jk}}}, \quad (20)$$

where $t_{11} = \tau_{12} = \tau_{21} N_1/N_2$, $t_{12} = t_{21} = \tau_{21} \sqrt{N_1/N_2}$, $t_{22} = \tau_{21}$ (in this section we label the σ band with 1 and π band with 2), Eq. (16) can be written as

$$\left[|2n-1| \begin{pmatrix} 1 & 0 \\ 0 & 1 \end{pmatrix} + \begin{pmatrix} G_{11} & -G_{12} \\ -G_{21} & G_{22} \end{pmatrix} \right] \begin{pmatrix} \delta_{1n} \\ \delta_{2n} \end{pmatrix} = \begin{pmatrix} \Lambda_{11} & \Lambda_{12} \\ \Lambda_{21} & \Lambda_{22} \end{pmatrix} \sum_{|\omega_m| \leq \Omega_m} \begin{pmatrix} \delta_{1m} \\ \delta_{2m} \end{pmatrix} \quad (21)$$

or, realizing that the right-hand side of (20) does not depend on the Matsubara index and denoting the elements of the corresponding 2×1 matrix with c_1 and c_2 , as

$$\begin{pmatrix} \Lambda_{11} & \Lambda_{12} \\ \Lambda_{21} & \Lambda_{22} \end{pmatrix} \sum_{|\omega_m| \leq \Omega_m} \left[|2m-1| \begin{pmatrix} 1 & 0 \\ 0 & 1 \end{pmatrix} + \begin{pmatrix} G_{11} & -G_{12} \\ -G_{21} & G_{22} \end{pmatrix} \right]^{-1} \begin{pmatrix} c_1 \\ c_2 \end{pmatrix} = \begin{pmatrix} c_1 \\ c_2 \end{pmatrix}. \quad (22)$$

The 2×2 matrix

$$\hat{G} = \begin{pmatrix} G_{11} & -G_{12} \\ -G_{21} & G_{22} \end{pmatrix} \quad (23)$$

is a real symmetric matrix, Eq. (19), with eigenvalues $d = G_{11} + G_{22}$ and 0 (see (19) and subsequent definitions of various t_{ij} parameters) and could be diagonalized through an orthogonal transformation

$$\hat{R} \hat{G} \hat{R}^{-1} = \begin{pmatrix} d & 0 \\ 0 & 0 \end{pmatrix}, \quad (24)$$

where the elements of \hat{R} are $R_{11} = \sqrt{G_{11}/(G_{11} + G_{22})}$, $R_{12} = -\sqrt{G_{22}/(G_{11} + G_{22})}$, $R_{21} = -R_{12}$ and $R_{22} = R_{11}$. Expressing \hat{G} in (21) in terms of the right-hand side of Eq. (23) and using

$$\sum_{|\omega_m| \leq \Omega_m} \frac{1}{|2m-1|+d} = \psi\left(\frac{\Omega_m}{2\pi T_c} + 1 + \frac{d}{2}\right) - \psi\left(\frac{1}{2} + \frac{d}{2}\right), \quad (25)$$

where ψ is the digamma function [26], Eq. (21) can be rewritten as

$$\hat{M} \begin{pmatrix} c_1 \\ c_2 \end{pmatrix} = \begin{pmatrix} c_1 \\ c_2 \end{pmatrix}, \quad (26)$$

where

$$\begin{aligned} \hat{M} = & \left[\psi\left(\frac{\Omega_m}{2\pi T_c} + 1\right) - \psi\left(\frac{1}{2}\right) \right] \begin{pmatrix} \Lambda_{11} & \Lambda_{12} \\ \Lambda_{21} & \Lambda_{22} \end{pmatrix} - \left[\psi\left(\frac{G_{11} + G_{22}}{2} + \frac{1}{2}\right) - \psi\left(\frac{1}{2}\right) \right] \\ & + \psi\left(\frac{\Omega_m}{2\pi T_c} + 1\right) - \psi\left(\frac{\Omega_m}{2\pi T_c} + 1 + \frac{G_{11} + G_{22}}{2}\right) \\ & \times \begin{pmatrix} \Lambda_{11} & \Lambda_{12} \\ \Lambda_{21} & \Lambda_{22} \end{pmatrix} \begin{pmatrix} \frac{G_{11}}{G_{11}+G_{22}} & \frac{-\sqrt{G_{11}G_{22}}}{G_{11}+G_{22}} \\ \frac{-\sqrt{G_{11}G_{22}}}{G_{11}+G_{22}} & \frac{G_{22}}{G_{11}+G_{22}} \end{pmatrix}. \end{aligned} \quad (27)$$

The transition temperature is the highest T_c for which the larger eigenvalue of \hat{M} is equal to 1.

We have solved Eqs. (25-26) for T_c as a function of the interband impurity scattering rate and our results are shown by the long dashed line in Fig. 1. The electron-phonon interaction parameters were taken to be the same as those used in section 2: $\lambda_{11} \equiv \lambda_{\sigma\sigma} = 1.017$, $\lambda_{12} \equiv \lambda_{\sigma\pi} = 0.212$, $\lambda_{22} \equiv \lambda_{\pi\pi} = 0.446$ and $\lambda_{21} \equiv \lambda_{\pi\sigma} = 0.155$. The maximum phonon energy was taken to be $\Omega_m = 75$ meV, which is roughly the position of the largest peak in $\alpha^2 F_{\sigma\sigma}$ (see Fig. 1 in Ref. [25]) and the values of $\mu^*(\omega_c)$ s from section 2.2 were scaled down using (11) to the new cutoff Ω_m to give $\mu_{11}^*(\Omega_m) \equiv \mu_{\sigma\sigma}^*(\Omega_m) = 0.139578$, $\mu_{22}^*(\Omega_m) \equiv \mu_{\pi\pi}^*(\Omega_m) = 0.139217$, $\mu_{12}^*(\Omega_m) = \mu_{21}^*(\Omega_m) = 0.027081$. Clearly, including the electron-phonon renormalization effects improves the BCS treatment considerably. However, we want to stress that θ - θ model gives the improved values *only* for the *reduced* quantity T_c/T_{c0} as a function of the *reduced* interband scattering rate $\gamma_{\pi\sigma}/T_{c0}$. The *absolute* values of T_c are not accurately predicted by θ - θ model (e.g. we get too large a value for T_{c0} of 143 K so that the usual weak coupling approximation $\psi(\Omega_m/(2\pi T_{c0}) + 1) - \psi(1/2) \approx \ln(2e^\gamma \Omega_m/(\pi T_{c0}))$, where γ is the Euler's constant, cannot be made).

4. Summary

We have calculated the change in the superconducting transition temperature of MgB_2 caused by interband nonmagnetic impurity scattering using the Eliashberg theory with realistic electron-phonon [16] and Coulomb repulsion [24] parameters for this compound. Our central result is given in Fig. 1. We find much slower rate of T_c suppression than what is obtained from the BCS approach [19] which ignores the renormalization and

damping effects associated with the electron-phonon interactions. For small interband scattering rates the strong coupling calculation gives about 4.5 times slower suppression rate of T_c than the BCS approach. Moreover, the strong coupling calculation indicates that it is unrealistic to expect the transition temperature of MgB_2 to ever drop below 60% of its maximum value as a result of impurity scattering and the 20% drop in T_c upon irradiation by fast neutrons [13] is certainly within our calculated range (20% drop in T_c is obtained with $\gamma_{\pi\sigma}$ of about $4k_B T_{c0}$, Fig. 1). Hence, the initial expectations based on the BCS treatment of the two-band model [19] that a dramatic suppression of T_c in MgB_2 with interband impurity scattering would provide the final “smoking gun” evidence for the two-band model was exaggerated.

Our calculation with θ - θ model (long dashed line in Fig. 1) clearly indicates that the main reason for the failure of the BCS approach to quantitatively account for the dependence of T_c/T_{c0} on $\gamma_{\pi\sigma}/T_{c0}$ in MgB_2 is that the BCS treatment leaves out the electron-phonon renormalization effects. One should keep in mind, however, that for other multiband systems with electron-phonon and Coulomb interactions different from those calculated [16,24] for MgB_2 one would have to recalculate T_c/T_{c0} as a function of interband scattering rate $\gamma_{\pi\sigma}/T_{c0}$ using Eliashberg equations from section 2.1 with the interaction parameters which are relevant to the multiband superconductor that is being considered.

Acknowledgments

This work has been supported in part by the Natural Sciences and Engineering Research Council of Canada. The author is grateful to O. Jepsen for providing the numerical values of $\alpha^2 F$ s for MgB_2 presented in [16] and to K. V. Samokhin, M. Reedyk and S. K. Bose for their interest in this work.

References

- [1] Souma S, Machida Y, Sato T, Takahashi T, Matsui H, Wang S-C, Ding H, Kaminski A, Campuzano J C, Sasaki S and Kadowaki K 2003 *Nature (London)* **423** 65
- [2] Chen X K, Konstantinović M J, Irwin J C, Lawrie D D and Franck J P 2001 *Phys. Rev. Lett.* **87** 157002
- [3] Szabó P, Samuely P, Kačmarčík J, Klein T, Marcus J, Fruchart D, Miraglia S, Marcenat C and Jansen A G M 2001 *Phys. Rev. Lett.* **87** 137005; Samuely P *et al.* 2003 *Physica C* **385** 244
- [4] Schmidt H, Zasadzinski J F, Gray K E and Hinks D G 2002 *Phys. Rev. Lett.* **88** 127002; 2003 *Physica C* **385** 221
- [5] Iavarone M, Karapetrov G, Koshelev A E, Kwok W K, Crabtree G W, Hinks D G, Kang W N, Choi E-M, Kim H J, H-J Kim and Lee S I 2002 *Phys. Rev. Lett.* **89** 187002; 2003 *Physica C* **385** 215
- [6] Gonnelli R S, Daghero D, Ummarino G A, Stepanov V A, Jun J, Kazakov S M and Karpinski J 2002 *Phys. Rev. Lett.* **89** 247004; Daghero D *et al.* 2003 *Physica C* **385** 255
- [7] Eskildsen M R, Kugler M, Tanaka S, Jun J, Kazakov S M and Karpinski J and Fischer Ø 2002 *Phys. Rev. Lett.* **89** 187003; Eskildsen M R *et al.* 2003 *Physica C* **385** 169
- [8] Takasaki T, Ekino T, Muranaka T, Fujii H and Akimitsu J 2002 *Physica C* **378-381** 229

- [9] Martinez-Samper P, Rodrigo J G, Rubio-Bollinger G, Suderow H, Vieira S, Lee S and Tajima S 2003 *Physica C* **385** 233
- [10] Wang Y, Plackowski T and Junod A, 2001 *Physica C* **355** 179
- [11] Bouquet F, Fisher R A, Phillips N E, Hinks D G and Jorgensen J D 2001 *Phys. Rev. Lett.* **87** 047001
- [12] Bouquet F, Wang Y, Sheikin I, Plackowski T, Junod A, Lee S and Tajima S 2002 *Phys. Rev. Lett.* **89** 257001
- [13] Wang Y, Bouquet F, Sheikin I, Toulemonde P, Revaz B, Eisterer M, Weber H W, Hinderer J and Junod A 2003 *J. Phys.: Condens. Matter* **15** 883
- [14] Angst M, Puzniak R, Wisniewski A, Jun J, Kazakov S M, Karpinski J, Roos J and Keller H 2002 *Phys. Rev. Lett.* **88** 167004
- [15] Mazin I I and Antropov V P 2003 *Physica C* **385** 49
- [16] Golubov A A, Kortus J, Dolgov O V, Jepsen O, Kong Y, Andersen O K, Gibson B J, Ahn K and Kremer R K 2002 *J. Phys.: Condens. Matter* **14** 1353
- [17] Markowitz D and Kadanoff L P 1963 *Phys. Rev.* **131** 563
- [18] Allen P B 1982 *Z. Phys. B - Condensed Matter* **47** 45
- [19] Golubov A A and Mazin I I 1997 *Phys. Rev. B* **55** 15146
- [20] Mazin I I, Andersen O K, Jepsen O, Dolgov O V, Kortus J, Golubov A A, Kuz'menko A B and van der Marel D 2002 *Phys. Rev. Lett.* **89** 107002
- [21] Erwin S C and Mazin I I 2003 *Phys. Rev. B* **68** 132505
- [22] McMillan W L 1968 *Phys. Rev.* **175** 537
- [23] Schopohl N and Scharnberg K 1977 *Solid State Commun.* **22** 371
- [24] Choi H J, Roundy D, Sun H, Cohen M L and Louie S G 2004 *Phys. Rev. B* **69** 056502
- [25] Mitrović B 2004 *Eur. Phys. J. B* **38** 451
- [26] Allen P B and Mitrović B 1982 *Solid State Physics* vol 37, ed H Ehrenreich, F Seitz and D Turnbull (New York: Academic) pp 1-92
- [27] Kong Y, Dolgov O V, Jepsen O and Andersen O K 2001 *Phys. Rev. B* **64** 020501(R)
- [28] Mitrović B and Carbotte J P 1981 *Solid State Commun.* **37** 1009